

Article

Petrographic, REE, fluid inclusion and stable isotope study of magnesite from the Upper Triassic Burano Evaporites (Secchia Valley, northern Apennines): contributions from sedimentary, hydrothermal and metasomatic sources

Stefano Lugli(✉) · Giulio Morteani · Dominique Blamart

S. Lugli

Dipartimento di Scienze della Terra, Università degli Studi di Modena e Reggio Emilia, Largo S. Eufemia 19, Modena, Italy

G. Morteani

Lehrstuhl für Angewandte Mineralogie und Geochemie, Technische Universität München, Lichtenbergstrasse 4, Garching, Germany

D. Blamart

Laboratoire des Sciences du Climat et de l'Environnement, Domaine du CNRS, Bat.12, Avenue de la Terrasse, Gif sur Yvette Cedex, France



E-mail: lugli.stefano@unimo.it

Received: 8 January 2001 / **Accepted:** 12 December 2001 / **Published online:**

Editorial responsibility: P. Lattanzi

Abstract. Sparry and microcrystalline magnesite are minor constituents of the Upper Triassic Burano Evaporite Formation of the northern Apennines in Italy. Petrography and geochemistry of magnesite suggest three modes of formation. (1) Evaporitic precipitation of stratified microcrystalline magnesite layers associated with sulfate and carbonate rocks. Most REE are below ICP-MS detection limits. $\delta^{18}\text{O}$ is +20.2 ‰ (SMOW) and $\delta^{13}\text{C}$ is -2.6 ‰ (PDB). (2) Hydrothermal infill of Fe-rich (9.78 wt%

FeO) lenticular sparry magnesite. This type of magnesite is characterized by very low LREE concentrations, whereas HREEs are relatively high. The fluid inclusion composition is NaCl-MgCl₂-H₂O, salinity is ~30 wt% NaCl equiv., and total homogenization temperatures range

from 204-309 °C; $\delta^{18}\text{O}$ is +17.5‰ and $\delta^{13}\text{C}$ is +1‰. (3) The partial or total replacement of dolostones by lenticular sparry magnesite. LREEs are lower in magnesite compared with the partly replaced dolostones. Magnesite yields $\delta^{18}\text{O}$ and $\delta^{13}\text{C}$ compositions of +17.3 to +23.6‰ and +0.5 to +1.4‰, respectively, whereas the partly replaced dolostones yield $\delta^{18}\text{O}$ and $\delta^{13}\text{C}$ values of +25.0 to +26.2 and +1.3 to +1.9, respectively. Complete replacement of dolostones produced massive lenticular sparry magnesite rock containing ooids and axe-head anhydrite relicts; LREEs are depleted compared to unaffected dolostones; $\delta^{18}\text{O}$ and $\delta^{13}\text{C}$ compositions range from +16.4 to +18.4‰ and +0.4 to +0.9‰, respectively. These data and the association between fracture-filling and replacive magnesite suggests a metasomatic system induced by hydrothermal circulation of hot and saline Mg-rich fluids. These processes probably occurred in the Oligocene-Miocene, when the Burano Formation acted as main detachment horizon for the Tuscan Nappe during the greenschist facies metamorphism of the Apuane complex. Thrusting over the Apuane zone produced large scale fluid flow focused at the Tuscan Nappe front. Sources of Mg-rich fluids were metamorphic reactions in the Apuane complex and dissolution of Mg-salts at the thrust front. Considering a maximum tectonic burial depth of 10 km, as inferred from the geometry of the chain, the pressure-corrected temperature of magnesite precipitation (380 to 400 °C) and the calculated fluid composition ($\delta^{18}\text{O}=+13.3\pm 1.2\text{‰}$) are in the range of the published Apuane metamorphic temperatures (300-450 °C) and fluid compositions ($\delta^{18}\text{O}=7\text{-}16\text{‰}$). The results of this study support the hydrothermal-metasomatic model for the formation of sparry magnesite deposits at the expense of dolostone units involved in thrusting and low-grade metamorphism, as proposed for the Northern Graywacke Zone (Alps) and the Eugui deposit (western Pyrenees).

Keywords. Apennines - Evaporites - Italy - Magnesite

Introduction

The origin of sparry magnesite hosted in carbonate rocks has been the subject of the so-called "magnesite controversy" (Kralik et al. 1989). Two main interpretations have been proposed during the last decades. Syngeneticists invoke deposition of magnesite in hypersaline environments or during diagenesis (Quémeneur 1975; Siegl 1984; Pohl 1990). In this case, sparry textures may form because of subsequent recrystallization of microcrystalline magnesite (Niedermayr et al. 1983), or directly by "sedimentary to early diagenetic processes" (Pohl 1990). Epigeneticists propose that magnesite formed by metasomatic replacement of a carbonate precursor (Kralik and Hoefs 1978; Morteani et al. 1983; Aharon 1988; Lugli et al. 2000), or by precipitation from hydrothermal fluids (Halfon and Marcé 1975). The "magnesite controversy" arose mainly because most important deposits are found in tectonized and metamorphosed terranes, where the syngenetic features may have been overprinted or obliterated.

In the Burano Formation from the Secchia Valley (northern Apennines) different types of sparry and microcrystalline magnesite are preserved (Lugli 1996b). Although the presence of magnesite has no economic value, the study of these different types may help in understanding the origin of important deposits, such as those located in the Austrian Alps and the Spanish Pyrenees. As a contribution to the "magnesite controversy" this paper discusses the petrography, geochemistry, stable isotope

compositions, and fluid inclusion data of the Burano magnesites in relation to the proposed genetic mechanisms.

Geological setting

In Tuscany, the Burano Formation lies at the base of a more than 2-km-thick carbonate-clastic Mesozoic sequence, the Tuscan Succession or Nappe. The Burano Formation was the main décollement horizon for the Tuscan Nappe during the NE-directed build-up of the northern Apennines chain and the development of the Alpi Apuane metamorphic complex, located to the SW of the study area (Carmignani and Kligfield 1990; Fig. 1a). The Alpi Apuane complex is a tectonic window where greenschist facies rocks are separated from the overlying Tuscan Nappe and Ligurian Units by the Burano Formation, now present as calcareous breccias and cataclasites formed by removal of the sulfate portion ("Calcare Cavernoso"). The age of this tectono-thermal event dates back at 27 Ma (Kligfield et al. 1986; 30 Ma for Carter et al. 1994; Upper Oligocene-Lower Miocene for Carmignani et al. 1994), with inferred metamorphic temperatures of ~350-400 °C (D1 phase; Kligfield et al. 1986). Since the Miocene, the compressional structures have been affected by a large-scale eastward-propagating tectonic extension. In the Apuane area, the Burano Formation acted again as a detachment horizon during this extensional phase (D2 phase, Carmignani and Kligfield 1990), which has been dated at 14-8 Ma (Giglia and Radicati di Brozolo 1970; Kligfield et al. 1986), with inferred temperature of 370-420 °C and pressure corresponding to burial depth of 8-10 km (Carmignani et al. 1994; Franceschelli et al. 1997). Peak temperatures of 380-500 °C have been documented by Di Pisa et al. (1985).

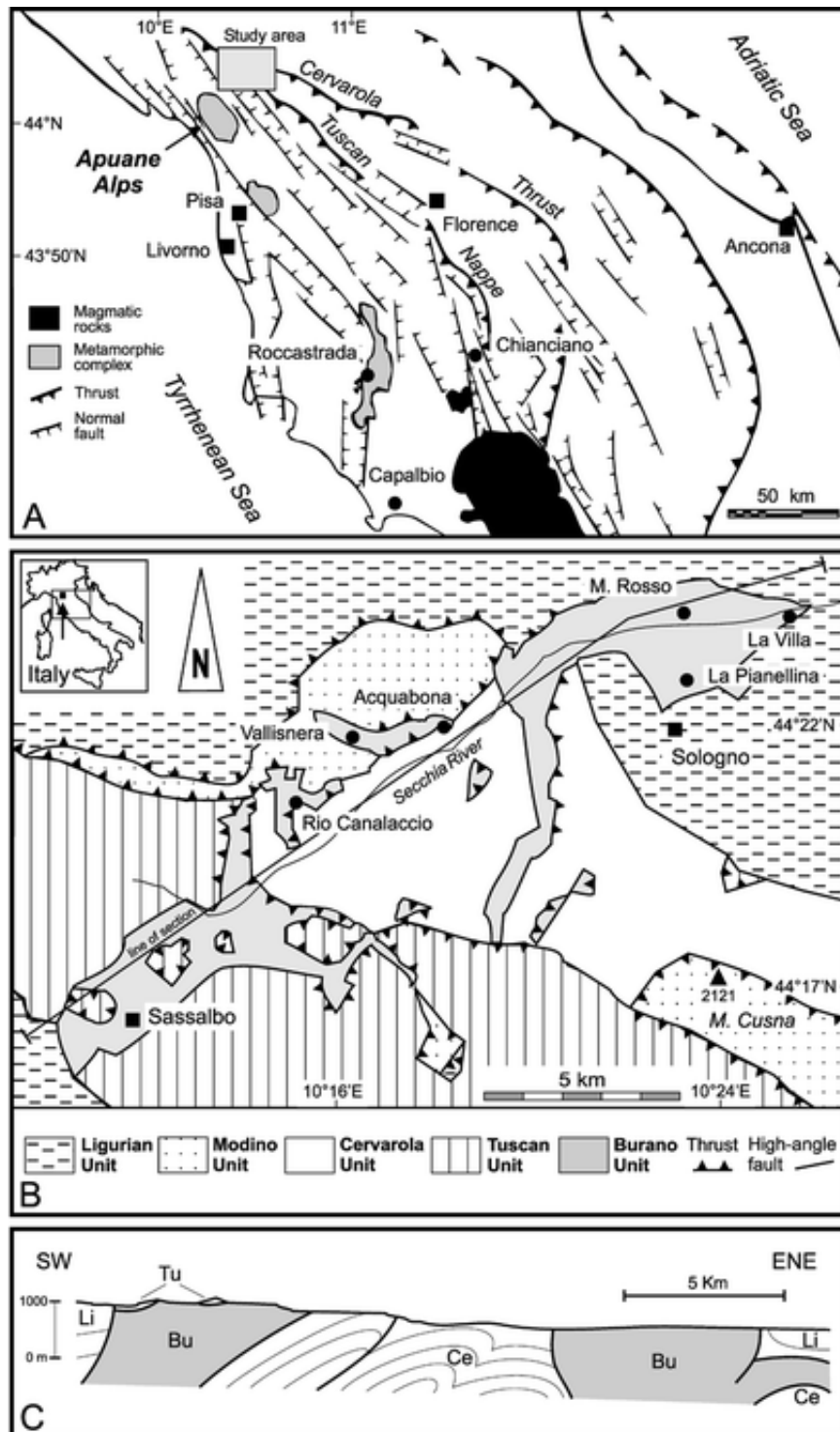


Fig. 1. **A** Simplified structural map of the northern Apennine chain showing the location of the study area and the Apuane metamorphic complex (simplified from Carmignani and Kligfield 1990). **B** Geological sketch of the study area of the Burano Evaporite Formation in the Secchia River Valley with sample locations (simplified from Andreozzi et al. 1987). **C** Geological cross section of the Secchia River valley (*line of section location* is shown in **B**). *Li* Ligurian Unit; *Tu* Tuscan Unit; *Bu* Burano Unit; *Ce* Cervarola Unit (simplified from Chicchi and Plesi 1991)

The Burano Formation in the Secchia Valley is exposed along a tectonic structure, which has been interpreted as a transpressional system running transverse to the major tectonic features of the northern Apennines, represented by the thrust fronts of the Tuscan Nappe and of the Tertiary Cervarola and Modino flysch units (Fig. 1a, b; Andreozzi et al. 1987). The evaporite unit is disrupted into thrust slices, which are tectonically displaced into younger allochthonous units. The evaporite thrust slices were detached from the base of the Tuscan Nappe by formation of mega-tension gashes. These thrust slices were then incorporated into the migrating overlying Ligurian units during a post-Lower Miocene deformation phase (Chicchi and Plesi 1991). Evidence that the Burano evaporites were affected by thermal events is (1) the presence of thrust slices composed of metasediments that correlate with the Apuane metamorphic complex (Calzolari et al. 1987), and (2) the widespread presence of authigenic quartz crystals with fluid inclusion homogenization temperatures ranging from 260 to 305 °C (Lugli 2001; see below).

The Burano Formation

The Upper Triassic Burano Formation from the Secchia Valley is mainly composed of meter- to decameter-scale alternating gypsum-anhydrite rocks and dolostones, which were affected by severe post-depositional modifications and strong tectonization. The inferred total thickness reaches 2,200 m in the northernmost zone (Colombetti and Fazzini 1986; M. Rosso, Fig. 1b).

Anhydrite can be found at depth, whereas gypsum prevails in the outcrops. The anhydrite rocks show flow structures, such as centimeter-scale pseudo-lamination consisting of transposed tight isoclinal folds outlined by comminuted dolostone fragments. The most common anhydrite texture is composed of aligned prismatic crystals. The gypsum rocks show the same general structures as the anhydrite rocks and are mostly composed of anhedral cloudy crystals. The gypsum rocks formed by alteration of anhydrite lithotypes by migration of sharp fronts propagating from fractures and strata boundaries (Lugli 2001).

The sulfate rocks contain idiomorphic black quartz crystals, which may reach several centimeters in size and are usually boudinaged (Lugli 1996a). The sigmoidal arrangement of their solid inclusions (mostly anhydrite and more rarely dolomite and magnesite) suggests that the main growth phases occurred during crystal rotation, possibly induced by the flow of the host anhydrite rock. These characteristics and the total homogenization temperatures of fluid inclusions ranging from 260 to 305 °C (Secchia Valley) and from 230 to 315 °C (Tuscany) indicate that some growth phases occurred at deep tectonic burial conditions (Lugli 2001). These conditions could be related to the evaporites acting as detachment horizon for the Tuscan Nappe during the Oligocene-Miocene development of the Apuane greenschist-facies metamorphic complex (Carmignani and Kligfield 1990).

As a consequence of the strong contrast in competence and "mobility", the carbonate layers frequently appear as megaboudins within a sulfate groundmass. The carbonate rocks are mainly massive dolomitic mudstones rarely showing cross stratification and lamination. The mudstones are composed of microcrystalline dolomite (dolomicrite) and commonly contain millimeter-scale nodules and triangular-, rectangular- or lenticular-shaped voids or bodies filled by microcrystalline dolomite after sulfate nodules and axe-head anhydrite. Rare dolomitized oolitic packstones and oolitic, pelletoidal, bioclastic grainstones have also been observed.

Although minor halite is only sparsely distributed at depth (Colombetti and Fazzini 1986; Lugli and Parea 1996), widespread and thick caprock-like sulfate megabreccias suggest the former presence of thick salt deposits (Lugli 2001).

The dissolution of the more soluble layers commonly produced a coarse, angular to spheroidal clast- or matrix-supported vuggy dolostone breccia ("Calcare cavernoso"; Vighi 1958; Passeri 1975). The vuggy aspect comes from the partial or total calcitization (de-dolomitization) of most dolostone clasts followed by calcite dissolution. In extreme cases, the rock has been transformed into a residual loose dolomite powder or sand called "Cenerone" (Passeri 1975).

Magnesite occurrence and petrography

The Burano Formation of the Secchia Valley is characterized by the presence of both microcrystalline and sparry magnesite (Lugli 1996b), but none was found in Tuscany, Umbria, and Marche in spite of careful searches of outcrops and boreholes. Magnesite has been found only as layer fragments or scattered crystals within dolomite and sulfate clasts floating in residual deposits or sulfate megabreccias produced by salt dissolution. The collected samples are small (centimeter- to meter-scale) and relatively rare, but the magnesite-bearing rocks are probably more widespread than observed because magnesite is a minor clastic constituent of karstic sediments (Bertolani and Rossi 1986). For these reasons, the cross cutting relationships among magnesite and the original host rocks are generally no longer recognizable, but the following petrographic criteria were useful reconstructing magnesite genesis:

1. The presence of primary fluid inclusions; fluid inclusion-rich magnesite crystals commonly grow from hydrothermal solutions (Tufar et al. 1989), whereas replacive magnesite is normally fluid inclusion-free (Möller 1989; Morteani 1989).
2. The composition of solid microinclusions in authigenic quartz crystals (see above); only dolomite is present within quartz crystals, even in those former dolomite rocks that have been completely replaced by magnesite. Magnesite microinclusions have been detected only within quartz crystals included in sulfate rocks containing microcrystalline magnesite layers. Therefore, microcrystalline magnesite pre-dates, whereas sparry magnesite post-dates, the metamorphic growth of the quartz euhedra. The main implication is that the origin of the microcrystalline magnesite is synsedimentary, or diagenetic.

The sparry magnesite crystals are dark or red depending on their iron content and degree of weathering. The sparry magnesite occurs as: (1) fracture-fillings, (2) scattered lens-shaped crystals in dolostones and sulfate rocks, and (3) massive rock.

1. The fracture-filling magnesite is relatively rare. The crystals are lens-shaped (3 cm in size), red to brown, and fill fractures up to 10 cm thick. These crystals are rich in primary fluid inclusions, a characteristic that suggests growth from hydrothermal solutions. At Acquabona, veins made of this type of magnesite were associated with sparry dolomite, chalcopyrite, and tennantite, and cut a dolostone containing scattered lens-shaped magnesite crystals (Figs. 2a and 3; the assemblage is shown in Fig. 4). The interstices of the vein are filled with late aragonite rosettes. This peculiar association is cut by later calcite veins.

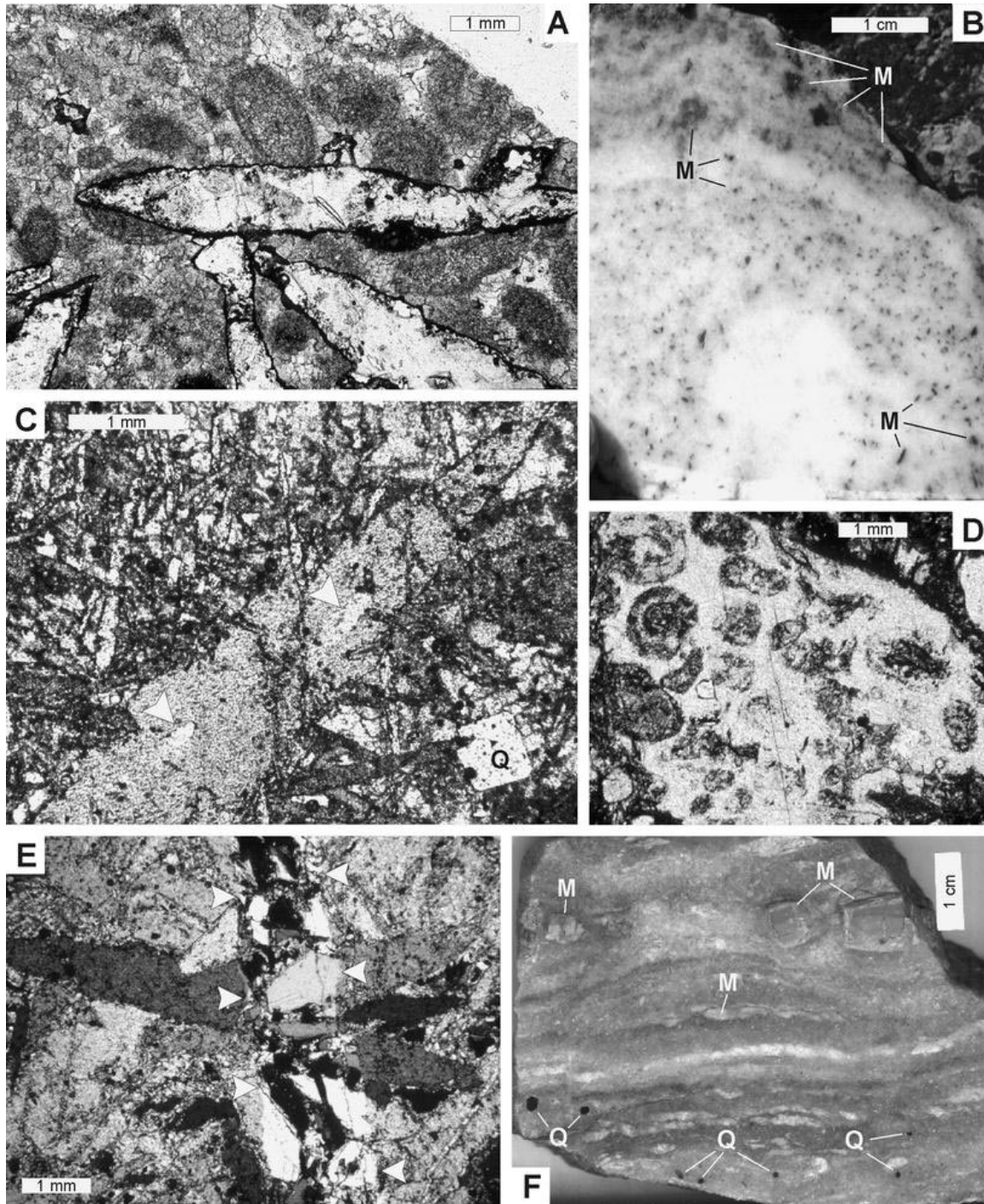


Fig. 2. **A** Thin-section photomicrograph of lenticular sparry magnesite replacing a dolomitic oolite rock. Note ooid and pellet ghosts within the magnesite. This replacive magnesite is associated with fracture-filling hydrothermal magnesite (see also Fig. 9). Sample SL AF DM (magnesite) and SL AF DD (dolostone). Acquabona (RE). Plane-polarized light (from Lugli 1996b). **B** Cut slab of a gypsum rock including small sparry magnesite lenses (*M*). Note that magnesite crystals form aggregates arranged in aligned spheroidal or prismatic bodies (*above*) resembling boudinaged and dismembered rock fragments. This type of magnesite appears to have replaced thin dolostone layer fragments. Sample SL 91, M. Rosso. **C** Thin-section photomicrograph of a massive rock composed of interlocked lenticular sparry magnesite. The large diagonal crystal includes bright axe-head shaped areas with anhydrite microrelicts (*arrows*). The rock contains authigenic quartz

crystals (*Q*) with dolomite microinclusions. Sample SL 1, La Villa. Plane-polarized light. (from Lugli 1996b). **D** Thin-section photomicrograph of a massive magnesite rock. The arrangement of impurities within a single magnesite crystal (*light gray*) indicates its origin by replacement of a former oolitic dolostone. Sample SL 28, La Pianellina. Crossed polars. **E** Thin-section photomicrograph of a massive magnesite rock. Note the fracture cutting the rock containing clear fluid inclusion-rich magnesite crystals (*arrowed*). The surrounding dark crystals are fluid inclusion-free. Some crystals in the two zones are in optical continuity. Sample SL 1, La Villa. Crossed polars. **F** Cut slab showing gray-colored microcrystalline magnesite boudins (*M*) in anhydrite rock. Note some authigenic quartz euhedra (*Q*) containing magnesite microinclusions. Sample SL 67, Rio Canalaccio (from Lugli 1996b)

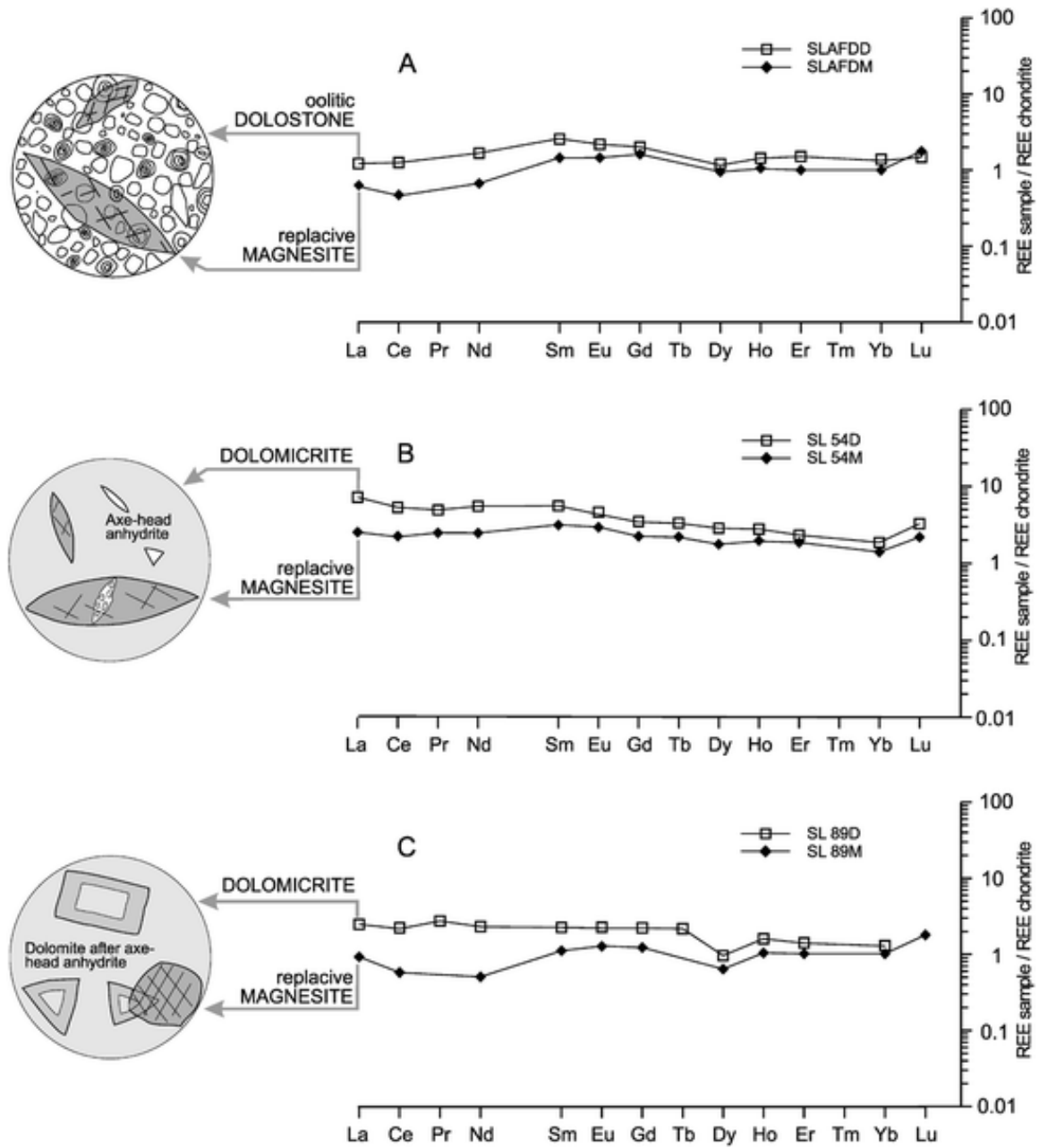


Fig. 3. REE patterns of replacive magnesite and its **A** oolitic dolostone and **B, C** dolomicrite precursors. Note the LREE-depleted patterns in magnesite. Chondrite composition after Sun and McDonough (1989)

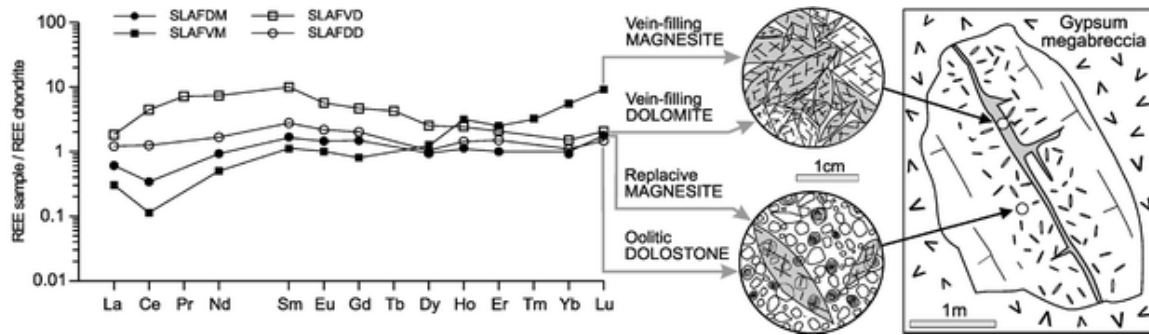


Fig. 4. Schematic diagram illustrating REE patterns of hydrothermal magnesite, hydrothermal dolomite, replacive magnesite and host dolostone at Acquabona. Chondrite composition after Sun and McDonough (1989)

2. The scattered lens-shaped magnesite crystals are hosted by:

- Oolitic dolostones (Figs. 2a and 3a) and dolomicrite rocks (Fig. 3b, c). The magnesite crystals are black, up to 3 cm across and devoid of primary fluid inclusions. The ooids and intraclasts of the host dolostones are commonly replaced by magnesite, but their shape is still recognizable within the magnesite crystals by the arrangement of opaque minerals, such as Fe-oxides/-hydroxides (Figs. 2a and 3a). Some magnesite crystals from dolomicrite rocks contain axe-head anhydrite relicts (Fig. 3b, c). Euhedral chalcopyrite has been identified in some samples. Some dolomicrites contain millimeter-sized nodules composed of partly leached calcite microspar. These patches may be interpreted as produced by de-dolomitization processes.
- Sulfate rocks (Fig. 2b). The magnesite crystals are lens-shaped, just a few millimeters in size, red, fluid inclusions-free, and can be undeformed or broken. These crystals are isolated or form aggregates arranged in aligned spheroidal, or prismatic bodies resembling boudinaged and dismembered rock fragments (Fig. 2b). This type of magnesite appears to have replaced thin dolostone layers broken into fragments. The magnesite formation by replacement of dolostone is supported by the presence of dolomite and the absence of magnesite inclusions in the associated authigenic quartz crystals.
- The massive sparry magnesite rocks are composed of black or red interlocked lenticular crystals up to 2 cm in size, which are devoid of primary fluid inclusions. The crystals show axe-head anhydrite inclusions (Fig. 2c) and ooid ghosts (Fig. 2d), suggesting that magnesite formed by replacement of dolostones. The authigenic quartz euhedra present in the massive magnesite rocks contain dolomite, but no magnesite inclusions (Fig. 2c), indicating that these rocks formed from a dolostone precursor. In one case (sample SL 1, Fig. 2e) the massive rock is cut by fractures containing zoned clear fluid inclusion-rich magnesite crystals, which are absent from the surrounding dark fluid inclusion-free crystals. The crystals in the two zones are in optical continuity. This suggests the same association between hydrothermal and replacive magnesite as previously described for the Acquabona example.

Microcrystalline magnesite rock forms centimeter-thick boudins within sulfate rocks (Fig. 2f). The fragments are gray, composed of crystals less than 15 μm in size and show a scanty layering, revealed by anhydrite and pyrite. The magnesite formation clearly predates the tectonic deformation of the host sulfate. The microcrystalline magnesite can thus be interpreted as the product of evaporite

precipitation or early diagenesis, as described for modern evaporite deposits (Schroll 1989). Such a mode of formation is supported by the presence of magnesite and the absence of dolomite microinclusions in the associated authigenic quartz crystals (Fig. 2f).

Geochemistry and microthermometry

Samples and analytical procedures

Nine representative samples of magnesite-bearing dolostone and sulfate rocks, and seven magnesite-free samples of dolostones of the Burano Formation from the Secchia Valley were selected for this study. A total of 24 mineral separates were hand picked for geochemical analysis on the basis of their mineralogy: magnesite (labeled M), dolomite (D), aragonite (AR), anhydrite (A), and gypsum (G). All samples were examined using optical microscopy and X-ray diffraction (XRD), and were analyzed for major, minor, and trace elements, including rare earth elements (REE). The carbonates were analyzed for carbon and oxygen stable isotopes and one magnesite sample was investigated for fluid inclusions.

For geochemical analysis, in order to eliminate calcite and dolomite from the magnesite, the samples were powdered, attacked with 37% HCl for several minutes until no reaction was recognizable, and then washed several times in distilled water. The same procedure was applied to the dolomite samples to eliminate the late calcite. In this case, the reaction was allowed to proceed only for a few seconds. Rare earth elements, U, Th, and Y were analyzed using a VG plasma quad inductively coupled plasma mass spectrometer (ICP-MS). All other elements were analyzed using inductively coupled plasma emission spectrometry (ICP-ES). A fusion procedure was used for digestion: 0.1 g of samples were mixed with 0.5 g of Na₂O₂ and sintered in a zirconium crucible at 560 °C. The sinter was dissolved in 40 ml of 7% HNO₃. Detection limit was 0.01 wt% for major elements and 10 ppm for minor elements. Detection limit for REE was 0.1 ppm, except Pr (0.2 ppm), Eu, Ho, and Lu (0.05 ppm).

Microthermometric analyses were performed with a Linkham freezing-heating stage on separate fragments of doubly-polished thin sections in order to avoid stretching phenomena produced by repeated heating-cooling cycles.

For stable isotope determinations, aliquots of ~15 mg of powdered samples were reacted under vacuum with anhydrous 100% phosphoric acid (McCrea 1950). Aragonite and calcite were attacked at 25 °C for 24 h, dolomite for over 72 h (Epstein et al. 1963), whereas magnesite was reacted at 50 °C for 72 h (Perry and Tan 1972; Aharon 1988). The extracted CO₂ was analyzed on a Finnigan Mat 251 mass spectrometer. Carbon and oxygen values are given in the conventional δ per mil notation relative to PDB and V-SMOW, respectively. Precision was better than ± 0.2 ‰. Values of 2.03 ‰ (Perry and

Tan 1972) and 0.83 ‰ (Friedman and O'Neil 1977) were subtracted from the measured $\delta^{18}\text{O}$ of

magnesite and dolomite, respectively, to correct for temperature-dependent fractionation between carbonates and phosphoric acid (Sharma and Clayton 1965; Aharon 1988). The calcite-water fractionation factor for oxygen isotopes has been taken from O'Neil et al. (1969). The dolomite-water fractionation factor has been obtained combining the calcite-water (O'Neil et al. 1969) with the dolomite-calcite fractionation of Sheppard and Schwarcz (1970). The latter factor has been preferred to that given by Matthews and Katz (1977) because it is empirically calibrated over a larger temperature range (100-650 °C). The magnesite-water oxygen isotope fractionation factor α is taken from Aharon (1988), extrapolated up to 450 °C and given as:

$$1000 \ln \alpha_{\text{magnesite-water}} = 3.53 \times 10^6 T^{-2} - 3.58$$

where T is the temperature in K.

For carbon, the calcite-CO₂ fractionation factor of Bottinga (1968) has been used and combined with the dolomite-calcite fractionation factor given by Sheppard and Schwarcz (1970) to obtain the dolomite-CO₂ fractionation factor, which can be expressed as follows:

$$1000 \ln \alpha_{\text{dolomite-CO}_2} = 3.2 \times 10^6 T^{-2} - 7.7103 T^{-1} + 2.6$$

The $\delta^{13}\text{C}$ values of the fluids calculated from the dolomite-H₂CO₃ fractionation factor (Ohmoto and Rye 1979) do not differ significantly from those calculated from the dolomite-CO₂ fractionation factor. In the absence of any available fractionation factor between magnesite and CO₂, this has been approximated to the dolomite-CO₂ fractionation factor (Aharon 1988).

Major and minor elements

The concentrations of selected elements of the Burano carbonates are listed in Table 1. The complete data set of all analyses can be obtained, upon request, from the corresponding author.

Table 1. Major and minor elements and stable isotope compositions of the Burano Formation rocks. Separates from a bulk sample have the same number. *M* Magnesite; *D* dolomite; *A* anhydrite; *G* gypsum; *AR* aragonite; *n.d.* not detected. *Blank* Not analyzed. Analyses performed by XRAL, Don Mills, Ontario. Stable isotopes - $\delta^{18}\text{O}$ per mil (SMOW); $\delta^{13}\text{C}$ per mil (PDB)

Sample	Type	Locality	SiO ₂	Al ₂ O ₃	FeO	MgO	CaO	K ₂ O	Mn	Cu	Sr	Th	U	Zn	$\delta^{18}\text{O}$	$\delta^{13}\text{C}$
			(%)	(%)	(%)	(%)	(%)	(%)	(ppm)	(ppm)	(ppm)	(ppm)	(ppm)	(ppm)		
Microcrystalline magnesite																
SL 67	Layer in anhydrite rock	Canalaccio	0.09	0.05	3.07	19.2	0.42	n.d.	1,140	n.d.	1,160	0.2	0.5	n.d.	+20.2	-2.6
Sparry magnesite																
SLAFVM	Hydrothermal vein-filling	Acquabona	0.01	n.d.	9.78	17.1	0.04	n.d.	1,950	n.d.	n.d.	0.2	n.d.	n.d.	+17.5	+1.0
SLAFDM	Replacing dolomicrite	Acquabona	1.44	0.02	5.74	18.7	0.16	0.01	1,370	22	n.d.	0.2	0.8	n.d.	+23.6	+1.4
SL 1	Massive rock (replacive)	La Villa	0.23	0.03	0.83	23.9	0.1	0.04	709	n.d.	n.d.	0.1	0.6	n.d.	+18.4	+0.4
SL 21	In gypsum rock	La Villa	0.23	0.08	4.57	19.7	1.08	0.05	1,750	n.d.	499	0.5	n.d.	14		
SL 28	Massive rock (replacive)	La Pianellina	0.6	0.07	3.66	22.5	0.13	0.03	673	n.d.	n.d.	0.2	0.4	n.d.	+16.4	+0.9
SL 54M 1	Replacing dolomicrite (core)	La Villa	1.41	0.5	1.02	25	0.25	0.49	804	n.d.	n.d.	1.1	0.5	96	+17.3	+0.6
SL 54M 2	Replacing dolomicrite (rim)	La Villa													+17.7	+0.0
SL 89M	Replacing dolomicrite	Vallisnera	0.23	0.07	2.52	22.6	0.11	0.08	1,510	64	n.d.	0.3	0.9	163	+17.4	+1.4

Sample	Type	Locality	SiO ₂	Al ₂ O ₃	FeO	MgO	CaO	K ₂ O	Mn	Cu	Sr	Th	U	Zn	δ_{18O}	δ_{13C}
			(%)	(%)	(%)	(%)	(%)	(%)	(ppm)	(ppm)	(ppm)	(ppm)	(ppm)	(ppm)		
SL 91	Crystals within gypsum rock	Mt. Rosso	0.21	0.04	7.25	18.9	0.41	0.02	1,820	n.d.	278	0.2	n.d.	n.d.	+20.4	-0.7
Dolomite																
SLAFDD	Partly-replaced dolomicrite	Acquabona	0.34	0.03	0.25	9.27	15.6	n.d.	263	n.d.	53	0.3	1.0	n.d.	+25.5	+1.7
SLAFVD	Hydrothermal vein-filling	Acquabona	n.d.	n.d.	1.52	10.6	18.4	n.d.	499	n.d.	137	n.d.	n.d.	n.d.	+20.0	-2.2
SL D	Dolomicrite	La Pianellina	0.13	0.04	0.16	9.13	14.4	0.03	62	n.d.	213	0.4	1.2	n.d.	+26.4	+3.2
SL 30	Dolomicrite	La Pianellina	0.14	0.02	0.05	11.4	18.1	0.05	25	n.d.	405	0.4	0.6	n.d.	+27.0	+3.0
SL 43	Dolomicrite	La Pianellina	1.64	0.23	0.62	11.2	18.2	0.09	176	n.d.	89	1.1	1.3	n.d.		
SL 44	Dolomicrite	La Pianellina													+25.8	+2.9
SL 54D	Partly-replaced dolomicrite	La Villa	1.56	0.47	0.48	10.8	17.9	0.43	119	n.d.	100	2.1	1.6	57	+26.2	+1.3
SL 89D	Partly-replaced dolomicrite	Vallisnera	0.27	0.08	0.23	10.5	17.7	0.1	143	103	69	0.4	1.3	24	+25.0	+1.9
SL 1 00	Dolomicrite	Roccastrada	0.52	0.21	0.09	12.1	20.4	0.05	20	n.d.	283	0.8	1.3	n.d.	+27.8	+4.5
SL 101	Dolomicrite	Capalbio	0.04	n.d.	0.02	11	17.7	0.01	14	n.d.	56	0.2	1.1	n.d.	+27.7	+3.0
SL 1 02	Dolomicrite	Chianciano													+28.8	+3.8
Sulfates																
SL 67A	Anhydrite rock	Canalaccio	0.06	n.d.	0.12	0.48	21.8	n.d.	29	n.d.	2,110	0.2	0.1	n.d.		
SL 91G	Gypsum rock	Mt. Rosso	0.2	0.02	0.02	0.03	16.8	n.d.	n.d.	n.d.	1,740	0.2	n.d.	n.d.		
Aragonite																
SLAFAR	Rosettes	Acquabona										0.2	2		+24.9	-0.6
Calcite																
SLAFDM	Late vein-filling	Acquabona													+24.4	-3.8
SL 0	De-dolomitized patches	La Pianellina													+22.8	-9.9
SL 1	Late vein-filling	La Villa													+22.4	-3.0

Sample	Type	Locality	SiO ₂	Al ₂ O ₃	FeO	MgO	CaO	K ₂ O	Mn	Cu	Sr	Th	U	Zn	δ _{18O}	δ _{13C}
			(%)	(%)	(%)	(%)	(%)	(%)	(ppm)	(ppm)	(ppm)	(ppm)	(ppm)	(ppm)		
SL 21	Late vein-filling	La Villa													+24.6	-1.1
SL 28	Late vein-filling	La Pianellina													+23.3	+0.4
SL 54D	De-dolomitized patches	La Villa													+22.8	-10.2
SL 54M 1	Late vein-filling	La Villa													+22.4	-3.2
SL 79	Late vein-filling	Mt. Rosso													+24.0	+0.1
SL 89D	De-dolomitized patches	Vallisnera													+23.3	-7.3
SL 91	Late vein-filling	Mt. Rosso													+24.5	-1.3

Silica and aluminum contents are comparable in replacive magnesite (0.23-1.44 and 0.22-0.5 wt%, respectively) and corresponding replaced dolomite (0.27-1.56 and 0.03-0.47 wt%, respectively), indicating that replacement occurred without impurities displacement, such as quartz and clay minerals, as documented for the Eugui magnesite (Lugli et al. 2000). As expected, the lowest SiO₂ and Al₂O₃ contents (<0.01 wt%) are those of vein-filling hydrothermal magnesite and dolomite.

The iron content reaches its maximum in vein-filling hydrothermal magnesite (9.78 wt%) and dolomite (1.52 wt%). Replacive magnesites contain more FeO (1.02-5.74 wt%) than the host dolostones (0.23-0.48 wt%). Microcrystalline magnesite contains small euhedral pyrite crystals and the measured 3.07 wt% FeO, thus, is mostly related to sulfide content.

Small amounts of CaO in replacive magnesite (0.10-0.13 wt%) indicate that the magnesite possibly contains residual microinclusions of dolomite. An exception is sample SL 54m, whose CaO content (0.25 wt%) is partly a result of axe-head anhydrite inclusions. As expected, the vein-filling hydrothermal magnesite has the lowest CaO content (0.04 wt%). Relatively high CaO concentrations in magnesite from sulfate rocks probably reflect the presence of gypsum/anhydrite inclusions, as in the case of samples containing 0.41-1.08 wt% CaO and 278-1,160 ppm Sr (SL 21, SL 67, and SL 91M).

As expected, strontium contents are below the detection limit for replacive magnesites (<10 ppm) because Sr can not enter the magnesite lattice (Möller 1989), whereas the replaced dolostones show values between 53 and 100 ppm. Magnesite-free dolostones may reach up to 405 ppm Sr.

Rare earth elements

The abundance of rare earth elements in magnesite is significantly low and close to detection limits. Concentration variations among associated carbonates, such as dolostones and replacive magnesite, are very small, but larger than analytical errors and, most importantly, display comparable trends for similar petrofacies. For these reasons, the REE distribution patterns provide reliable information on magnesite genesis.

As a whole, magnesite shows chondrite-normalized patterns very similar to those of dolostones, but LREE contents of magnesite are significantly lower, whereas HREEs show comparable concentrations (Fig. 3).

Figure 4 relates the REE distribution patterns of the peculiar carbonate association of the Acquabona outcrop to the respective petrographic features. The REE pattern of vein-filling hydrothermal dolomite is very similar to that of the host dolostone, but REE contents are higher in dolomite (Fig. 4). The vein-filling magnesite shows the lowest LREE and the highest HREE contents. REE patterns of replacive magnesite and its host oolitic dolostone are very similar, but magnesite is significantly depleted in LREEs (Fig. 4).

As summarized in Fig. 5, all magnesite and dolostone samples show REE patterns rather similar in shape, although magnesite is slightly LREE-depleted.

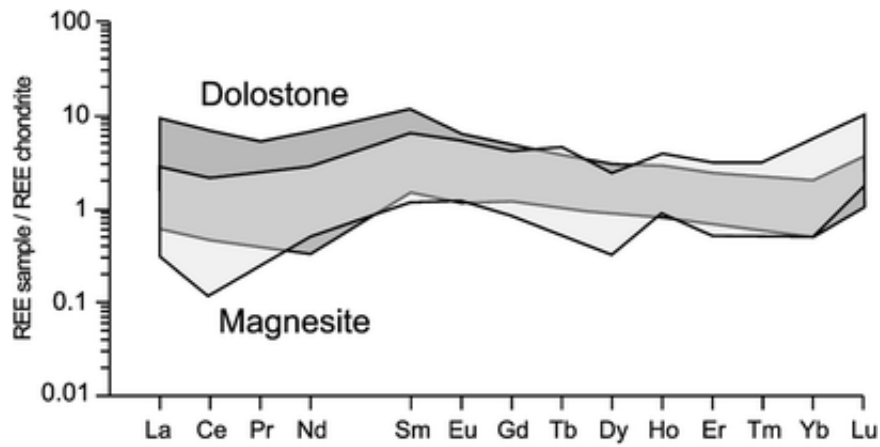


Fig. 5. REE patterns of dolostone and magnesite samples from the Burano Formation. Note the LREE-depleted pattern of magnesites. Chondrite composition after Sun and McDonough (1989)

A comparison of the REE patterns in sulfate-hosted magnesites with those in massive magnesites is depicted in Fig. 6a. Magnesite in sulfate rocks displays rather similar patterns as replacive (Fig. 3) and massive magnesites, but REE concentrations are lower in massive magnesites (most HREEs are below detection limit).

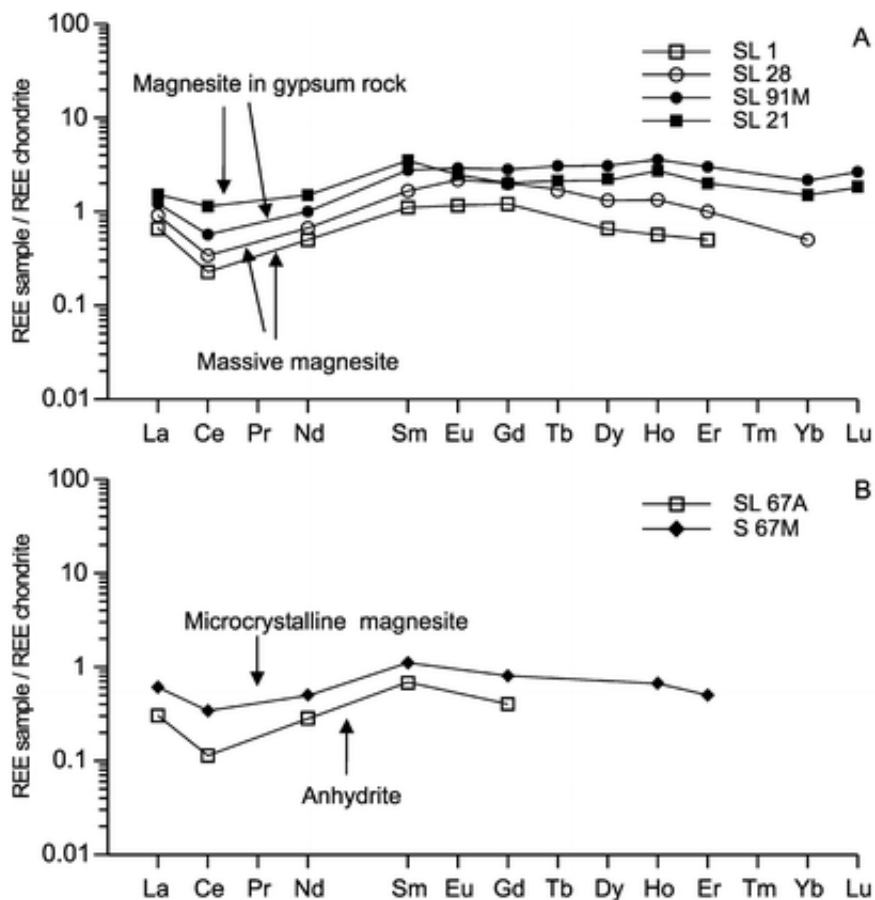


Fig. 6. **A** REE patterns of magnesite in sulfate rocks compared with massive sparry magnesite rocks, and **B** REE patterns of microcrystalline magnesite compared with its anhydrite host rock. Chondrite composition after Sun and McDonough (1989)

The REE patterns of microcrystalline magnesite and its anhydrite host rock are characterized by very low REE contents and most elements are below detection limit (Fig. 6b). As discussed above, this sample is slightly contaminated by anhydrite and pyrite; thus the true magnesite REE concentrations are probably even lower than the measured values.

Fluid inclusions

Fluid inclusions have been observed only in the vein-filling sparry magnesite from Acquabona (sample SL AF VM, Fig. 4). Spatially, the inclusions are either grouped in clusters along cleavage planes or may be relatively isolated. More rarely, planes or trails of inclusions were also observed. All inclusions are small, and generally not larger than 10 μm . Most inclusions have negative crystal shapes (rhombohedra), although irregular shapes were also observed. The inclusions form two homogeneous populations based on composition: liquid + vapor and liquid + vapor + solid. The solid phase always displays a cubic shape and is probably halite. Two-phase inclusions with irregular elongated shapes were not considered in this study because of their suspect necking-down textures (Roedder 1984).

Because of the small inclusion size, problems were encountered during freezing runs in observing the multiple, complex phase transitions. In particular, detection of first ice melting was extremely difficult. The temperatures at which this phase change became evident was between -37.9 and -29.4 $^{\circ}\text{C}$,

indicating NaCl-MgCl₂-H₂O as the major chemical components of the fluid (Davis et al. 1990). Ice disappeared between -36 and -29.4 °C. On a particularly large inclusion it was possible to observe also the presence of birefringent crystals, possibly a hydrated salt phase such as hydrohalite, which melted at -12.4 °C. Using the equation of state of Brown and Lamb (1989), these data indicate a fluid salinity of about 29-30 wt% NaCl equiv.

Upon heating, the inclusions homogenized to the liquid phase, and the vapor to liquid homogenization temperatures ranged from 120 to 318 °C. Melting of halite daughter crystals ranged from 204 to 309 °C (Fig. 7).

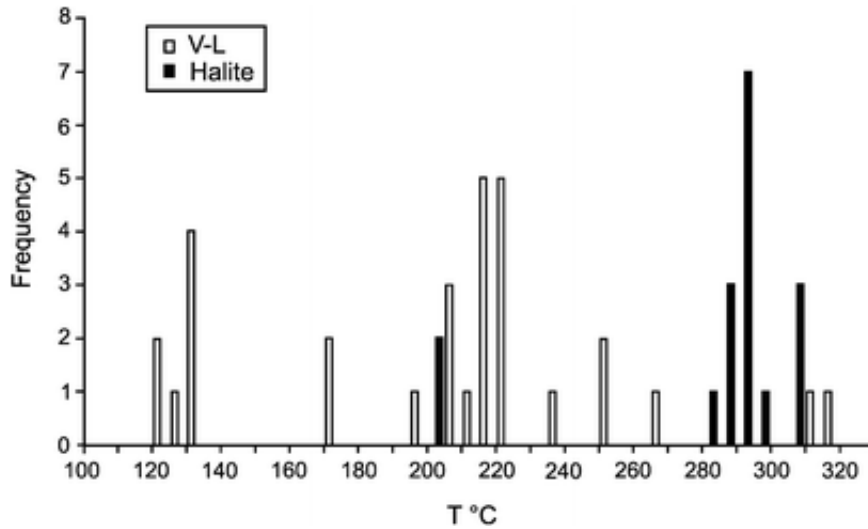


Fig. 7. Frequency histogram relating vapor to liquid homogenization temperatures (V-L) and halite melting temperatures (halite) for fluid inclusions in fracture-filling sparry magnesite from Acquabona (RE). Sample SL AF VM

Assuming 10 km as the maximum burial depth of the Burano Formation during the Apennine tectogenesis, as deduced from the model of Carmignani and Kligfield (1990), pressure-corrected temperatures may be estimated for the corresponding lithostatic load of 2.7 GPa. Using the equation of state of Brown and Lamb (1989), pressure-corrected maximum trapping temperatures of 380 to 400 °C are calculated.

Stable isotopes

The stable isotope composition of carbonates from the Burano Formation is listed in Table 1 and plotted in Fig. 8. The sparry magnesite values ($\delta^{18}\text{O}=16.4\text{-}23.6\text{‰}$ and $\delta^{13}\text{C}=-0.7$ to 1.4‰) are in the range of those reported by Kralik et al. (1989) for other world occurrences ($\delta^{18}\text{O}=6.5\text{-}25.3\text{‰}$ and $\delta^{13}\text{C}=-7.5$ to 5.8‰).

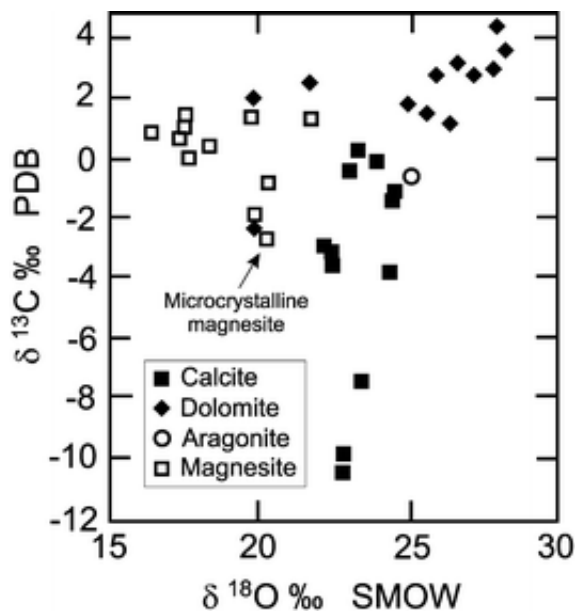


Fig. 8. Carbon and oxygen isotope plot of magnesite, dolomite, calcite, and aragonite from the Burano Formation

Relatively homogeneous $\delta^{18}\text{O}$ values characterize hydrothermal magnesite (17.5‰), massive sparry rocks ($17.4 \pm 1\text{‰}$) and magnesite replacing dolostone ($17.5 \pm 0.2\text{‰}$). An exception is sample SL AF DM (replacive magnesite), which shows an enrichment of $\sim 4\text{‰}$ relative to other sparry magnesites. No significant oxygen isotope variation has been observed between core (17.3‰) and rim (17.7‰) of magnesite crystals (sample SL 54M).

Corresponding $\delta^{13}\text{C}$ values are also homogeneous, in the range of 0.0 to 1.4‰ .

Magnesite in sulfate rocks and microcrystalline magnesite are enriched by $\sim 2.5\text{‰}$ relative to the hydrothermal magnesite. Magnesite in sulfate rocks and microcrystalline magnesite show the lowest $\delta^{13}\text{C}$ values (-0.7 and -2.6‰).

Magnesite-free dolostones show homogeneous isotopic compositions ($\delta^{18}\text{O} = 27.4 \pm 0.8\text{‰}$ and $\delta^{13}\text{C} = 3.6 \pm 0.9\text{‰}$; Table 1; Fig. 8). These values are typical of Triassic dolostones (Veitser and Hoefs 1976; Land 1979) and are similar to the metamorphosed Grezzoni dolostones (mean $\delta^{18}\text{O} = 28.1\text{‰}$,

$\delta^{13}\text{C}=2.8\text{‰}$) and to the "Calcare Cavernoso" ($\delta^{18}\text{O}=24.8\text{--}26.2\text{‰}$, $\delta^{13}\text{C}=-5.8$ to 3.2‰) from the Apuane Alps (Cortecci et al. 1992).

Dolostones partly replaced by sparry magnesite yield $\delta^{18}\text{O}$ values ranging from 25.0 to 26.2‰ (mean 25.7‰) and $\delta^{13}\text{C}$ values ranging from 1.3 to 2.9‰ (mean 2.5‰). These

samples are depleted by $\sim 1.7\text{‰}$ in $\delta^{18}\text{O}$ and 1.0‰ in $\delta^{13}\text{C}$ relative to the magnesite-free

dolostones. These isotopic compositions are still compatible with marine dolomites, but the negative shift may indicate that the rocks have interacted with the fluids responsible for sparry magnesite formation. The vein-filling dolomite shows the most ^{18}O -depleted value (-2.2‰).

Late calcite veins cutting magnesite have homogeneous $\delta^{18}\text{O}$ values in the range of 22.2 to 24.6‰,

in contrast with the corresponding $\delta^{13}\text{C}$ values ranging from -3.7 to $+0.4\text{‰}$. The values of the one

aragonite sample ($\delta^{18}\text{O}=24.9$, $\delta^{13}\text{C}=-0.6\text{‰}$) also plot in the field of the late calcite veins. Calcite

formed through de-dolomitization shows similar $\delta^{18}\text{O}$ values (22.8–23.3‰), but $\delta^{13}\text{C}$ values are strongly depleted (-10.2 to -7.3‰).

Discussion

Hydrothermal magnesite and Mg-metasomatism of dolostones

The peculiar association in the Acquabona outcrop, where sparry magnesite veins cut a dolostone containing replacive magnesite, demonstrates that Mg-rich fluids produced hydrothermal magnesite but also permeated the country rock inducing the formation of replacive sparry magnesite at its expense. All the studied replacive magnesites contain significant amounts of Ca and are richer in Fe, Mn, and Zn than their partially replaced dolomitic precursor. This suggests that magnesite was produced by pervasive Mg-metasomatism of dolostones by fluids carrying appreciable amounts of Fe, Mn, and Zn. The final step of such a metasomatic process would be the complete transformation of the original dolostone into a massive sparry magnesite rock, which may contain veins of fluid inclusion-rich magnesite crystals similar to the described examples (samples SL 1 and 28). These hypotheses are supported by the REE patterns of sparry magnesite, which are not typical of sedimentary magnesite, but are most probably inherited from a dolostone precursor. Magnesite crystals typically grow incorporating mainly HREEs, whereas LREEs are rejected (Bau and Möller 1992). It follows that magnesite showing detectable amounts of LREEs may contain microinclusions of Ca-bearing minerals, suggesting replacement of a dolomite precursor (Möller 1989). In some cases, the LREE content may be inherited from impurities of the precursor, which were not displaced by magnesite growth (Lugli et al. 2000). All studied sparry magnesite samples contain CaO and LREEs and display petrographic features revealing their origin by dolostone replacement. Dolomite microinclusions are probably present in magnesite crystals because of incomplete dolostone replacement. An exception is the vein-filling magnesite, which is practically CaO- and LREE-free,

suggesting direct growth from hydrothermal solutions. The hydrothermal magnesite shows lower LREE and higher HREE contents compared with the replacive magnesite. Such a counterclockwise rotation of the pattern is typical of minerals produced from fluids that lost their LREE content because of the difference in REE complexation properties (Morteani et al. 1982, 1983; Hatzl and Morteani 1993).

The Mg-metasomatism of dolostones releases significant amounts of Ca and Sr into the fluids. This is because the strontium originally present in the dolostones cannot replace the smaller Mg^{2+} ion in the magnesite lattice (Möller 1989). The released Ca and Sr were possibly responsible for late deposition of calcite and aragonite.

In the Acquabona example, the negative fractionation between hydrothermal magnesite, hydrothermal dolomite, and replaced dolostone indicates an oxygen isotope disequilibrium. This isotopic disequilibrium can be caused by: (1) temperature effect, (2) change in isotopic composition of the fluids, (3) combination of these two effects, or (4) a partial isotopic exchange between fluids and minerals. To test these hypotheses, the isotopic composition of the fluid in equilibrium with hydrothermal magnesite was calculated using the fluid inclusion trapping temperatures (400 ± 50 °C) and the isotope data of the carbonates (Fig. 9). In this range of temperature, fluids in equilibrium with hydrothermal magnesite ($\delta^{18}O = 13.3 \pm 1.2$ ‰ and $\delta^{13}C = 2.7 \pm 0.2$ ‰) show different isotopic

values than those in equilibrium with dolomite ($\delta^{18}O = 16.0 \pm 1.2$ ‰ and $\delta^{13}C = -0.5 \pm 0.2$ ‰). It

follows that the two minerals cannot have precipitated from the same fluid. If the oxygen isotope composition of fluids in equilibrium with magnesite ($\delta^{18}O = 13.3 \pm 1.2$ ‰) was the same during

crystallization of dolomite, then the formation temperature was ~ 300 °C. At this temperature, the calculated $\delta^{13}C$ value of the fluid in equilibrium with dolomite (-1.0 ‰) is depleted by

$\sim 3-4$ ‰ relative to magnesite (2.7 ± 0.2 ‰). This discrepancy and the relatively depletion in $\delta^{13}C$

suggest that precipitation of hydrothermal dolomite took place in the presence of isotopically-light carbon, which possibly originated from decarboxylation of organic-rich sediments (Fallick et al. 1991; Zedef et al. 2000).

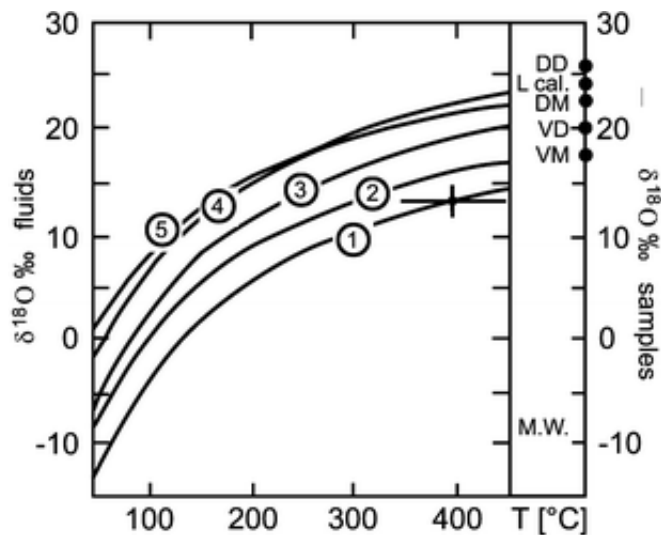


Fig. 9. Calculated $\delta^{18}\text{O}$ of fluids in equilibrium with the different carbonates in the Aquabona association (Fig. 4). 1 $\delta^{18}\text{O}$ of fluids in equilibrium with hydrothermal magnesite (VM sample SL AF VM); 2 $\delta^{18}\text{O}$ of fluids in equilibrium with hydrothermal dolomite (VD sample SL AF VD); 3 $\delta^{18}\text{O}$ of fluids in equilibrium with magnesite replacing dolostone (DM sample SL AF DM); 4 $\delta^{18}\text{O}$ of fluids in equilibrium with dolostone (DD SL AF DD); 5 $\delta^{18}\text{O}$ of fluids in equilibrium with the late calcite (L cal late vein-filling calcite in sample SL AF DM.); M.W. $\delta^{18}\text{O}$ of modern meteoric water in the studied area (Longinelli and Cortecci 1970). The cross represents fluid inclusions homogenization temperatures of hydrothermal magnesite (sample SL AF VM)

The sparry magnesite that replaced the dolostone was precipitated from fluids, which, at 400 °C, show isotope values similar to those calculated for hydrothermal magnesite ($\delta^{18}\text{O}=13.2\pm 1.4\text{‰}$ and $\delta^{13}\text{C}=2.4\pm 0.9\text{‰}$, Fig. 9). This indicates that both magnesite types may have crystallized at a similar temperature from fluids having similar isotopic composition. In contrast, at 400 ± 50 °C, the Acquabona replacive magnesite is in oxygen isotopic equilibrium with fluids ($\delta^{18}\text{O}=18.5\pm 1.2\text{‰}$) that are enriched by $\sim 5.5\text{‰}$ relative to the associated hydrothermal magnesite and to the other replacive magnesites. The $\delta^{13}\text{C}$ value of magnesite replacing dolostone ($2.9\pm 0.2\text{‰}$) is similar to that of the other replacive magnesite. If the oxygen isotope equilibrium (complete exchange) between sparry magnesite and hydrothermal fluids ($13.2\pm 1.4\text{‰}$) was attained, then the crystallization temperature was ~ 230 °C (Fig. 9).

The massive magnesite rocks seem to represent an intermediate case between magnesite replacing dolostones and magnesite in sulfate rocks. The equilibrium temperatures among these samples and a fluid with $\delta^{18}\text{O}\sim 13.4\pm 1.4\text{‰}$ are 330-400 °C (SL 1) and 400-450 °C (SL 28), and are still

compatible with those described for the other magnesite types. The similarity of $\delta^{13}\text{C}$ values among massive magnesite rocks and replacive magnesites suggests that they formed from a dolostone

precursor, as indicated also by the petrographic and chemical features.

The carbon isotopic fractionation between dolomite and calcite (and the one aragonite sample) is too large to represent isotopic equilibrium. Considering that dolostone $\delta^{13}\text{C}$ values are relatively homogeneous, the isotopic disequilibrium reflects the $\delta^{13}\text{C}$ heterogeneous composition of the calcite. The depleted calcite values can be explained in two ways. The first one could be a temperature effect. In this case, the isotopic equilibrium was with a fluid having $\delta^{13}\text{C} = -8.0\text{‰}$ over a temperature range of 30 to 450 °C. This hypothesis seems unlikely because (1) the calcite $\delta^{18}\text{O}$ values show a narrow range (2.4‰), suggesting that such a large temperature interval was not achieved, and (2) the oxygen fractionation gives temperatures of 60 °C (sample SL D), 70 °C (SL 54), 180 °C (SL 89D) and 220 °C (SL AF DD). As calculated for these temperatures, the $\delta^{13}\text{C}$ values of the fluids in equilibrium with calcite do not match the value of -8‰ (an exception is sample SL 89D), suggesting that the calcite carbon isotope compositions evolved independently from those of dolostones. It follows that the calcite $\delta^{13}\text{C}$ -depleted values cannot be explained by a temperature effect or by a fractionation effect because carbon isotope fractionation among dolomite and carbon species is small (Ohmoto and Rye 1979). The broad $\delta^{13}\text{C}$ composition range of late calcites possibly originated by interaction of "normal" carbonate rocks ($\delta^{13}\text{C} = 0 \pm 2\text{‰}$) with various contributions of low $\delta^{13}\text{C}$ values ($-10 \pm 2\text{‰}$). These low carbon isotope values indicate a contribution of carbonate from decarboxylation of organic-rich sediments (Fallick et al. 1991; Zedef et al. 2000).

Regarding oxygen, the dolomite-calcite thermometer yields temperatures between 60 and 220 °C. The calculated $\delta^{18}\text{O}$ values of the fluids are 0.6 and 15.8‰, respectively. Two main implications can be deduced from these data. First, at low temperature the fluids have a light oxygen isotope composition, probably of meteoric origin. Second, the $\delta^{18}\text{O}$ fluid values in equilibrium with calcite and dolomite at 220 °C are similar to those in equilibrium with the associated magnesite.

Sedimentary magnesite

The petrographic characteristics indicate that microcrystalline magnesite pre-dates the tectonic deformation and the precipitation of the metamorphic quartz euhedra, suggesting a sedimentary origin. The sedimentary origin of the Burano microcrystalline magnesite is also supported by its very low REE concentration, similar to present-day fine-grained Mg-carbonates forming in evaporite deposits (Schroll 1989). This is because seawater is characterized by a low REE/Mg, and REE tend to co-precipitate with Ca-minerals before magnesite saturation is reached. For these reasons, when magnesite starts to precipitate, seawater is practically devoid of lanthanides (Möller 1989). However, the measured $\delta^{18}\text{O}$ value of the Burano microcrystalline magnesite is depleted by ~10-20‰ relative to modern analogues ($\delta^{18}\text{O} = 30\text{-}40\text{‰}$; Kralik et al. 1989). At 50 °C, fluids in equilibrium with microcrystalline magnesite would have a calculated $\delta^{18}\text{O}$ of about -10‰, which is incompatible with seawater. It follows that fine-grained magnesite equilibrated at elevated temperature. At 400 °C,

fluids in equilibrium with fine-grained magnesite have $\delta^{18}\text{O}$ and $\delta^{13}\text{C}$ values of $16.0 \pm 1.2\text{‰}$ and $-0.8 \pm 0.2\text{‰}$, respectively (Fig. 9). At 400 °C, fluids in equilibrium with sparry magnesite in sulfate rocks and microcrystalline magnesite yield similar calculated $\delta^{18}\text{O}$ and slightly different $\delta^{13}\text{C}$ values (1.2 to $-0.2 \pm 0.2\text{‰}$). This suggests that fine-grained magnesite and sparry magnesite in sulfate rocks probably equilibrated under similar temperature conditions and isotopic fluid compositions. The absence of recrystallization textures in fine-grained magnesite (i.e., sparry crystals) may indicate that (1) the oxygen isotope exchange was a diffusive process with a probably low water/rock ratio, and (2) fluid-free conditions prevailed after isotope exchange, possibly because of the low permeability of the host sulfate rocks. By contrast, high water/rock ratios prevailed during formation of sparry magnesite at the expense of dolostones.

Constraints for sparry magnesite formation

The transition from the stability field of dolomite to that of magnesite can be produced by temperature increase and/or by decrease of the Ca/Ca+Mg ratio in the fluids in equilibrium with dolomite (Johannes 1970; Morteani et al. 1983). Considering that some of the largest sparry magnesite deposits are located at the front of thrust sheets, Morteani and Neugebauer (1990) suggested that magnesite replacement of dolostones can be produced during thrusting by fluid movement as consequence of squeezing of hot vadose and pore waters from underlying units and dehydration reactions in the lower tectonic unit.

Because hydrothermal-metasomatic magnesite is present only in the Secchia Valley, at the northernmost thrust front of the Tuscan Nappe (Fig. 1), the model proposed by Morteani and Neugebauer (1990) appears to be applicable. The fluid movement could have been induced by the northern Apennine tectogenesis, when the Burano Formation acted as main detachment horizon for the Tuscan Nappe during the Apuane Complex metamorphism (Oligocene-Miocene; Fig. 10). This hypothesis is supported by the calculated $\delta^{18}\text{O}$ values of the fluids, which cannot have a meteoric or seawater-derived origin. A magmatic origin seems also unlikely because no magmatic activity occurred in the studied area during the Apennine tectogenesis. The probable source of fluids were the metamorphic reactions occurring in the Apuane Complex. Isotopically heavy fluids similar to those responsible for magnesite formation ($\delta^{18}\text{O} = 13.3 \pm 1.2\text{‰}$) have been calculated for the Apuane metamorphism ($\delta^{18}\text{O} = 7\text{--}16\text{‰}$; Benvenuti et al. 1991).

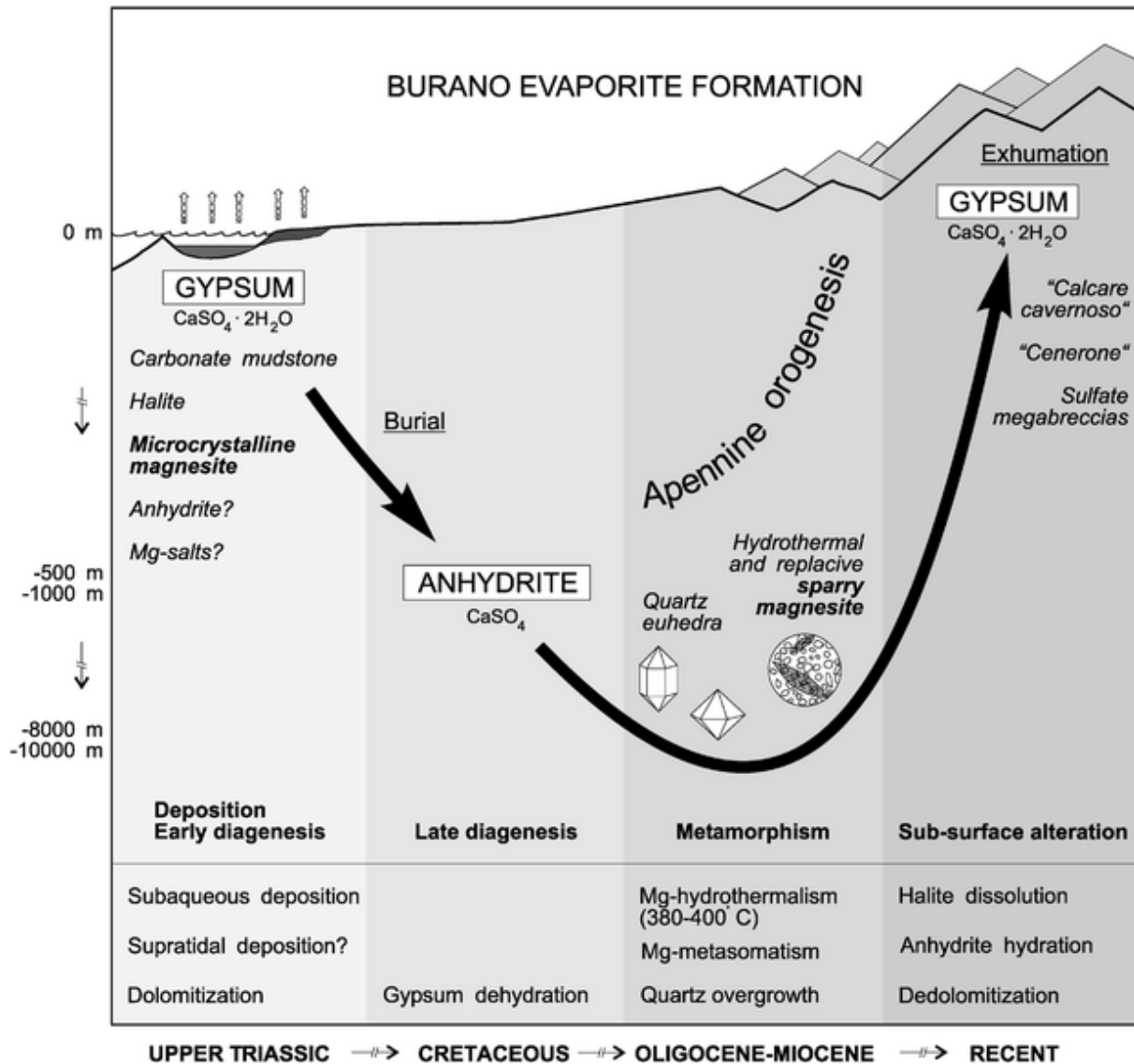


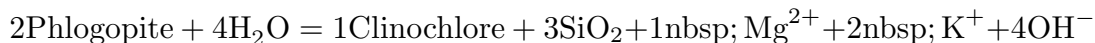
Fig. 10. Summary diagram showing the geologic history of the Burano Formation (modified from Lugli 2001)

The calculated temperatures for magnesite formation (380 to 400 °C) are in the range of the estimated Apuane fluid temperatures (300 to 450 °C; Cortecchi et al. 1989, 1992).

It is not clear at present at which stage of the metamorphism the sparry magnesite may have formed. Fluids with high salinity (14.5-24.5 wt% NaCl equiv.) similar to that measured in the magnesite (29-30 wt% NaCl equiv.) were attributed to the D2 phase of the Apuane metamorphism (Costagliola et al. 1999). High salinity fluids within the Burano Evaporite Formation, however, would be expected for most part of its geologic history, probably during both D1 and D2 phases.

The source of magnesium necessary for dolomite metasomatism may have been:

1. Metamorphic reactions in pelitic sediments of the Apuane complex. Morteani et al. (1982) report the following typical Mg-producing reactions:



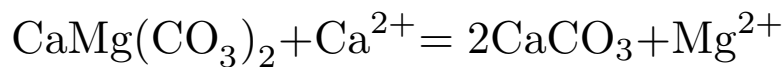
The observation that pyrophyllite is a common mineral in the Apuane metamorphic rocks (Franceschelli et al. 1986, 1997) suggests that significant amounts of Mg may have been produced during its formation.

2. Dissolution of Mg-rich salts (such as kieserite, polyhalite, bischofite, carnallite, epsomite, and kainite). The replacement of dolostones by magnesite may occur by the following reaction (Johannes 1970):



The only Mg-mineral in the Burano Formation is polyhalite $\text{Ca}_2\text{MgK}_2(\text{SO}_4)_4 \cdot 2\text{H}_2\text{O}$, which has been observed in drill-cores from Tuscany, although not in the Secchia Valley. On the other hand, the former presence of large halite masses, now vanished into residual deposits and cap-rock megabreccias, has been documented at the thrust front (M. Rosso, Fig. 1; Lugli 2001). The possibility that Mg-salts were present at the thrust front in association with halite cannot be excluded and would explain the $\text{NaCl-MgCl}_2\text{-H}_2\text{O}$ fluid inclusion composition of hydrothermal magnesite.

3. Calcitization of dolostones (de-dolomitization). De-dolomitization processes may produce a significant Mg-enrichment in the fluids, as indicated by the reaction:



These processes commonly occurred in Tuscany (Vighi 1958; Passeri 1975) and in the Secchia Valley, where large masses of "Calcarea cavernoso" and "Cenerone" residual rocks have been produced by selective leaching of replacive calcite. De-dolomitization processes may be produced by both meteoric-derived fluids at low P_{CO_2} (De Groot 1967) and/or thermal decomposition of organic matter (Clark 1980). Petrographic evidence, however, indicates that alteration of dolostones occurred at late near-surface conditions (Lugli 2001), which appear incompatible with the described fluid inclusion and stable isotope data.

4. Remobilization of former sedimentary magnesite during the Apuane metamorphism.

Conclusions

The presence of three different types of magnesite in the Burano Formation of the northern Apennines provided a unique opportunity to study their petrography and geochemistry in order to constrain mode and time of formation.

Microcrystalline magnesite was probably deposited in the Upper Triassic hypersaline environment in association with sulfate and halite. In the Oligocene-Miocene, the evaporite sequence became the detachment horizon of the Tuscan Nappe, which overthrust the Apuane zone (Fig. 10). Thrusting produced large-scale fluid movement focused at the Tuscan Nappe front. The source of Mg-rich fluids was mostly the metamorphic reactions occurring in the Apuane complex, but magnesium content was possibly further enhanced by leaching of Mg-salts located at the thrust front. The Mg-rich fluids

deposited hydrothermal magnesite in veins and induced at the same time the partial or total Mg-metasomatic replacement of dolostones by sparry magnesite at estimated temperatures as high as 400 °C. At these high temperatures, the synsedimentary microcrystalline magnesite was isotopically re-equilibrated but did not recrystallize to form sparry textures. This suggests that formation of sparry magnesite from sedimentary microcrystalline magnesite (Quémeneur 1975; Niedermayr et al. 1983; Siegl 1984), or during early diagenesis (Pohl 1990), is unlikely. The results of this study support the hydrothermal-metasomatic model for the formation of sparry magnesite (Halfon and Marcé 1975; Kralik and Hoefs 1978; Morteani et al. 1983; Aharon 1988). The example of the Burano Formation in the northern Apennines indicates that sparry magnesite may form at expense of dolostone units involved in thrust tectonics and low-grade metamorphism, as proposed for the northern Greywacke Zone in the Alps (Morteani and Neugebauer 1990) and the Eugui deposit in the western Pyrenees (Lugli et al. 2000).

Acknowledgements. We thank C. Preinfalk for help with preparation of drawings and K. Holzhäuser for analytical assistance with the C and O isotope determinations. We thank M. Russell, W. Pohl, and P. Lattanzi for a critical review of the manuscript.

References

- Aharon P (1988) A stable-isotope study of magnesites from the Rum Jungle uranium field, Australia: implications for the origin of strata-bound massive magnesites. *Chem Geol* 69:127-145
- Andreozzi M, Casanova S, Chicchi S, Ferrari S, Patterlini PE, Pesci M, Zanzucchi G (1987) Riflessioni sulle evaporiti triassiche dell'alta Val Secchia (RE). *Mem Soc Geol It* 39:69-75
- Bau M, Möller P (1992) Rare earth element fractionation in metamorphogenic hydrothermal calcite, magnesite and siderite. *Mineral Petrol* 45:231-246
- Benvenuti M, Costagliola P, Lattanzi P, Cortecchi G, Tanelli G (1991) A genetic model of polymetallic ore deposits from Apuane Alps: evidences from stable isotope data. In: Paget M, Leroy L (eds) *Source, transport and deposition of metals*, Balkema, Rotterdam, pp 249-252
- Bertolani M, Rossi A (1986) La petrografia del Tanone Grande della Gaggiolina (154 E/RE) nelle evaporiti dell'Alta Val Secchia (Reggio Emilia - Italia). *Le Grotte d'Italia* (4)XII 1984/85:79-105
- Bottinga Y (1968) Calculation of fractionation factors for carbon and oxygen exchange in the system calcite-carbon dioxide-water. *J Phys Chem* 72:800-808
- Brown PE, Lamb WM (1989) P-V-T properties of fluid inclusions in the system $H_2O \pm CO_2 \pm NaCl$. New graphical presentation and implications for fluid inclusions studies. *Geochim Cosmochim Acta* 53:1209-1221
- Calzolari MA, Ferrari S, Patterlini PE, Zanzucchi G (1987) Segnalazione di metasedimenti tra le evaporiti triassiche dell'alta Val Secchia (RE). *Mem Soc Geol It* 39:77-81
- Carmignani L, Kligfield R (1990) Crustal extension in the northern Apennines: the transition from compression to extension in the Alpi Apuane core complex. *Tectonics* 9:1275-1303
- Carmignani L, Cerrina Feroni A, Del Tredici S, Fantozzi PL, Giglia G, Martinelli P, Meccheri M, Robbiano A (1994) Considerazioni sul profilo La Spezia - Reggio Emilia. *Studi Geologici Camerti Spec Vol* (1992/2) appendice CROP 1-1A:17-29

- Carter KE, Dworking SI, Carmignani L, Meccheri M, Fantozzi P (1994) Dating thrust events using $^{87}\text{Sr}/^{86}\text{Sr}$: an example from the northern Apennines, Italy. *J Geol* 102:297-305
- Chicchi S, Plesi G (1991) Sedimentary and tectonic lineations as markers of regional deformation: an example from the Oligo-Miocene arenaceous flysch of the Northern Apennines. *Boll Soc Geol It* 110:601-616
- Clark DN (1980) The diagenesis of Zechstein carbonate sediments. In: Fuechtbauer H, Peryt T (eds) *The Zechstein Basin with emphasis on carbonate sequences*. *Contrib Sedimentol* 9:167-203
- Colombetti A, Fazzini P (1986) Il salgemma nella formazione dei gessi triassici di Burano (Villaminozzo, RE). *Le Grotte d'Italia* (4) XII 1984/85:209-219
- Cortecchi G, Lattanzi P, Tanelli G (1989) Sulfur, oxygen and carbon isotope geochemistry of barite-iron oxide-pyrite deposits from Apuane Alps (northern Tuscany, Italy). *Chem Geol* 76:249-257
- Cortecchi G, Benvenuti M, Lattanzi P, Tanelli G (1992) Stable isotope geochemistry of carbonates from the Apuane alps mining district, northern Tuscany, Italy. *Eur J Mineral* 4:509-520
- Costagliola P, Benvenuti M, Maineri C, Lattanzi P, Ruggieri G (1999) Fluid circulation in the Apuane Alps core complex: evidence from extension veins in the Carrara marble. *Mineral Mag* 63:111-122
- Davis DW, Lowenstein TK, Spencer R (1990) Melting behavior of fluid inclusions in laboratory-grown halite crystals in the systems $\text{NaCl-H}_2\text{O}$, $\text{NaCl-KCl-H}_2\text{O}$, $\text{NaCl-MgCl}_2\text{-H}_2\text{O}$, and $\text{NaCl-CaCl}_2\text{-H}_2\text{O}$. *Geochim Cosmochim Acta* 54:591-601
- De Groot K (1967) Experimental dedolomitization. *J Sediment Petrol* 37:1216-1220
- Di Pisa A, Franceschelli M, Leoni L, Meccheri M (1985) Regional variation of the metamorphic temperatures across the Tuscanidi I Unit and its implications on the Alpine metamorphism (Apuane Alps, N. Tuscany). *N Jahrb Mineral Abh* 151:197-211
- Epstein S, Graf DL, Degens ET (1963) Oxygen isotope studies on the origin of dolomites. In: Craig H, Miller SL, Wasserburg GT (eds) *Isotopic and cosmic chemistry*. North Holland, pp 169-180
- Fallick AE, Ilich M, Russell MJ (1991) A stable isotopic study of the magnesite deposits associated with the Alpine-type ultramafic rocks of Yugoslavia. *Econ Geol* 86:847-891
- Franceschelli M, Leoni L, Memmi I, Puxeddu G (1986) Regional distribution of Al-silicates and metamorphic zonation in the low-grade Verrucano metasediments from the Northern Apennines, Italy. *J Metamorph Geol* 4:309-321
- Franceschelli M, Memmi I, Carcangiu G, Gianelli G (1997) Prograde and retrograde chloritoid zoning in low temperature metamorphism, Alpi Apuane, Italy. *Schweiz Mineral Petrogr Mitt* 77:41-50
- Friedman I, O'Neil JR (1977) Compilation of stable isotope fractionation factors of geochemical interest. In: Fleischer M (ed) *Data of geochemistry*. Ch KK US Geol Surv, Prof Pap 440-KK 1-12
- Giglia G, Radicati di Brozolo R (1970) K/Ar age of metamorphism in the Apuane Alps (Northern Tuscany). *Boll Soc Geol It* 89:485-497

Halfon J, Marcé A (1975) Compositions isotopiques en carbon et oxygène de la magnésite de Serre de Motner et autres carbonates associés dans la série de Canaveilles (Pyrénées-orientales): Consequences génétiques. CR Acad Sci Paris 280:1521-1524

Hatzl T, Morteani G (1993) Secondary redistribution of REE, Ba, Sr, and Mn in intrusive and extrusive carbonatites. Terra Nova (abstr suppl) 3:5-21

Johannes W (1970) Zur Entstehung von Magnesitvorkommen. N Jb Min Abh 113:274-325

Kligfield R, Hunziker J, Dallmeyer RD, Schamel S (1986) Dating of deformation phases using K-Ar and $^{40}\text{Ar}/^{39}\text{Ar}$ techniques: results from the Northern Apennines. J Struct Geol 8:781-798

Kralik M, Hoefs J (1978) Die Isotopenzusammensetzung der Karbonate in der Magnesitlagerstätte Egui (Westpyrenäen). Tschermaks Mineral Petrogr Mitt 25:185-193

Kralik M, Aharon P, Schroll E, Zachmann D (1989) Carbon and oxygen isotope systematics of magnesites: a review. In: Möller P (ed) Magnesite: geology, mineralogy, geochemistry, formation of Mg-carbonates. Monogr Ser Mineral Deposits 28:197-223

Land LS (1979) Isotopic and trace element geochemistry of dolomite: the state of the art. Am Assoc Petrol Geol Bull 63(3):485

Longinelli A, Cortecchi G (1970) Isotopic abundance of oxygen and sulfur in sulfate ions from river waters. Earth Planet Sci Lett 7:376-380

Lugli S (1996a) Petrography of the quartz euhedra as a tool to provide indications on the geologic history of the Upper Triassic Burano Evaporites (Northern Apennines, Italy). Mem Soc Geol It 48:61-65

Lugli S (1996b) The magnesite in the Upper Triassic Burano Evaporites of the Secchia River valley (Northern Apennines, Italy): petrographic evidence of an hydrothermal-metasomatic system. Mem Soc Geol It 48:669-674

Lugli S (2001) Timing of post-depositional events in the Burano Formation of the Secchia Valley (Upper Triassic, northern Apennines), clues from gypsum-anhydrite transitions and carbonate metasomatism. Sediment Geol 140:107-122

Lugli S, Parea GC (1996) Halite cube casts in the Triassic sandstones from the upper Secchia River valley (Northern Apennines, Italy). Environmental interpretation. Acc Naz Sci Lett Arti Modena 15:341-351

Lugli S, Torres-Ruiz J, Garuti G, Olmedo Rojas F (2000) Petrography and geochemistry of the Eugui magnesite deposit (Western Pyrenees, Spain), evidence for the development of a peculiar zebra banding by dolomite replacement. Econ Geol 95:1775-1791

Matthews A, Katz A (1977) Oxygen isotope fractionation during the dolomitization of calcium carbonate. Geochim Cosmochim Acta 41:1431-1438

McCrea JM (1950) On the isotopic chemistry of carbonates and a paleotemperature scale. J Chem Phys 18(6):849-857

- Möller P (1989) Minor and trace elements in magnesite. In: Möller P (ed) Magnesite: geology, mineralogy, geochemistry, formation of Mg-carbonates. Monogr Ser Mineral Deposits 28:173-196
- Morteani G (1989) Fluid inclusions in magnesite. In: Möller P (ed) Magnesite: geology, mineralogy, geochemistry, formation of Mg-carbonates. Monogr Ser Mineral Deposits 28:237-240
- Morteani G, Neugebauer H (1990) Chemical and tectonic controls on the formation of sparry magnesite deposits - the deposits of the northern Greywacke Zone (Austria). Geol Rundsch 79(2):337-344
- Morteani G, Möller P, Schley F (1982) The rare earth element contents and the origin of the sparry magnesite mineralizations of Tux-Lanersbach, Entachen Alm, Spiessnägel, and Hochfilzen, Austria, and the lacustrine magnesite deposits of Aiani-Kozani, Greece, and Bela Stena, Yugoslavia. Econ Geol 77:617-631
- Morteani G, Schley F, Möller P (1983) On the formation of magnesite. In: Schneider HJ (ed) Mineral deposits of the Alps and of the Alpine Epoch in Europe. Springer, Berlin Heidelberg New York, pp 97-104
- Niedermayr G, Beran A, Scheriau-Niedermayr E (1983) Magnesite in Permian and scythian series of the eastern Alps, Austria, and its petrographic significance. In: Schneider HJ (ed) Mineral deposits of the Alps and of the Alpine Epoch in Europe. Springer, Berlin Heidelberg New York, pp 105-115
- Ohmoto H, Rye RO (1979) Isotopes of sulfur and carbon. In: Barnes HL (ed) Geochemistry of hydrothermal ore deposits, 2nd edn. Wiley-Interscience, New York, pp 509-567
- O'Neil JR, Clayton RN, Mayeda TK (1969) Oxygen isotope fractionation in divalent metal carbonates. J Chem Phys 51:5547-5558
- Passeri L (1975) L'ambiente deposizionale della formazione evaporitica nel quadro della paleogeografia del Norico Tosco-Umbro-Marchigiano. Boll Soc Geol It 94:231-268
- Perry EC, Tan FC (1972) Significance of oxygen and carbon isotope determinations in early Precambrian cherts and carbonate rocks in southern Africa. Bull Geol Soc Am 83:687-664
- Pohl W (1990) Genesis of magnesite deposits - models and trends. Geol Rundsch 79(2):291-299
- Quémeneur J (1975) Assay d'interprétation synthétique de la formation de magnésite en milieu sédimentaire: application aux gisements du pays basque. Proc Congr Intl Sedimentol 9:169-179
- Roedder E (1984) Fluid inclusions. Rev Mineral Mineral Soc Am 12:644
- Schroll E (1989) Recent formation of magnesite in evaporitic environment. The example of the Coorong Lagoon (South Australia). In: Möller P (ed) Magnesite: geology, mineralogy, geochemistry, formation of Mg-carbonates. Monogr Ser Mineral Deposits 28:29-34
- Sharma T, Clayton RN (1965) Measurements of $^{18}\text{O}/^{16}\text{O}$ and $^{13}\text{C}/^{12}\text{C}$ ratios of carbonates gneisses, serpentinites and marbles of the Zillertaler Alps, western Tauern area (Austria). N Jahrb Mineral Monatsh 10:444-459
- Sheppard SMF, Schwarcz HP (1970) Fractionation of carbon and oxygen isotopes and magnesium between coexisting metamorphic calcite and dolomite. Contrib Mineral Petrol 26:161-198

Siegl W (1984) Reflections on the origin of sparry magnesite deposits. In: Wauschkuhn A, Kluth C, Zimmermann RA (eds) Syngeneses and epigenesis in the formation of mineral deposits. Springer, Berlin Heidelberg New York, pp 177-182

Sun S-S, McDonough WF (1989) Chemical and isotopic systematics of oceanic basalts: implications for mantle composition and processes. In: Saunders AD, Norry MJ (eds) Magmatism in the ocean basins. Geol Soc Spec Publ 42:313-345

Tufar W, Glemb J, Schmidt R, Möller P, Pohl W, Riedler H, Olsacher A (1989) Formation of magnesite in the Radenthein (Carinthia/Austria) type locality. In: Möller P (ed) Magnesite: geology, mineralogy, geochemistry, formation of Mg-carbonates. Monogr Ser Mineral Deposits 28:135-172

Veitzer J, Hoefs J (1976) The nature of $^{18}\text{O}/^{16}\text{O}$ and $^{13}\text{C}/^{12}\text{C}$ secular trends in sedimentary carbonate rocks. Geochim Cosmochim Acta 40:1387-1395

Vighi L (1958) Sulla serie triassica "Cavernoso-Verrucano" presso Capalbio (Orbetello - Toscana) e sulla brecciatura tettonica delle serie evaporitiche, "Rocce madri" del Cavernoso. Boll Soc Geol It 78(1):221-236

Zedef V, Russell M J, Fallick A E, Hall AJ (2000) Genesis of vein stockwork and sedimentary magnesite and hydromagnesite deposits in the ultramafic terranes of southwestern Turkey: a stable isotope study. Econ Geol 95:429-446